NIH Public Access
Author Manuscript
Circulation. Author manuscript; available in PMC 2014 April 28.

Published in final edited form as:
Circulation. 2009 November 10; 120(19): 1883–1892. doi:10.1161/CIRCULATIONAHA.108.837724.

Glycome and Transcriptome Regulation of Vasculogenesis

Rania Harfouche, PhD[#], **Dirk M. Hentschel, MD**[#], **Stephanie Piecewicz, BS**[#], **Sudipta Basu, PhD**, **Cristin Print, MBChB, PhD**, **David Eavarone, BS**, **Tanyel Kiziltepe, PhD**, **Ram Sasisekharan, PhD**, and **Shiladitya Sengupta, PhD**

Department of Medicine (R.H., D.M.H., S.P., S.B., S.S.), Brigham and Women's Hospital, Boston, Mass; Department of Molecular Medicine and Pathology (C.P.), University of Auckland, Auckland, New Zealand; Department of Biological Engineering (D.E., T.K., R.S.), Massachusetts Institute of Technology, Cambridge, Mass; and Harvard-MIT Division of Health Sciences and Technology (R.H., S.P., S.B., D.E., T.K., R.S., S.S.), Cambridge, Mass.

[#] These authors contributed equally to this work.

Abstract

Background—Therapeutic vasculogenesis is an emerging concept that can potentially be harnessed for the management of ischemic pathologies. The present study elucidates the potential coregulation of vasculogenesis by the heparan sulfate glycosaminoglycan–rich cell-surface glycome and the transcriptome.

Methods and Results—Differentiation of embryonic stem cells into endothelial cells in an in vitro embryoid body is paralleled by an amplification of heparan sulfate glycosaminoglycan sulfation, which correlates with the levels of the enzyme *N*-deacetylase/*N*-sulfotransferase 1 (NDST1). Small hairpin RNA–mediated knockdown of NDST1 or modification of heparan sulfate glycosaminoglycans in embryonic stem cells with heparinases or sodium chlorate inhibited differentiation of embryonic stem cells into endothelial cells. This was translated to an in vivo zebrafish embryo model, in which the genetic knockdown of NDST1 resulted in impaired vascularization characterized by a concentration-dependent decrease in intersegmental vessel lumen and a large tail-vessel configuration, which could be rescued by use of exogenous sulfated heparan sulfate glycosaminoglycans. To explore the cross talk between the glycome and the transcriptome during vasculogenesis, we identified by microarray and then validated wild-type and NDST1 knockdown–associated gene-expression patterns in zebrafish embryos. Temporal analysis at 3 developmental stages critical for vasculogenesis revealed a cascade of pathways that may mediate glycocalyx regulation of vasculogenesis. These pathways were intimately connected to cell signaling, cell survival, and cell fate determination. Specifically, we demonstrated that forkhead box O3A/5 proteins and insulin-like growth factor were key downstream signals in this process.

© 2009 American Heart Association, Inc.

Correspondence to Dirk M. Hentschel and Shiladitya Sengupta, Room 317, 65 Landsdowne St, Cambridge, MA 02139. shiladit@mit.edu or dhentschel@partners.org.

The online-only Data Supplement is available with this article at http://circ.ahajournals.org/cgi/content/full/CIRCULATIONAHA.108.837724/DC1. Guest Editor for this article was Daniel I. Simon, MD.

Disclosures

NIH-PA Author Manuscript
NIH-PA Author Manuscript
NIH-PA Author Manuscript

NIH-PA Author Manuscript

NIH-PA Author Manuscript

NIH-PA Author Manuscript

Conclusions—The present study for the first time implicates interplay between the glycome and the transcriptome during vasculogenesis, revealing the possibility of harnessing specific cellular glyco-microenvironments for therapeutic vascularization.

Keywords

neovascularization; physiological; embryonic stem cells; zebrafish; vasculature; signal transduction; IGF-2

Promotion of neovasculature holds the potential for ameliorating coronary artery disease, which is the leading cause of morbidity and mortality in the United States.[1] Although the focus has been on inhibiting angiogenesis in tumors, therapeutic angiogenesis is emerging as an exciting frontier in cardiovascular medicine, as recently articulated by Ferrara and Kerbel.[2] Indeed, physiological revascularization is essential for embryogenesis and tissue regeneration, such as that which occurs during wound healing, during ischemia, or after tissue transplantation.

The formation of neovasculature proceeds through 2 distinct processes: vasculogenesis, the development of the primordial vasculature de novo, and angiogenesis, the development of vasculature from an existing network.[3] The prevalent dogma was that neovasculature in the adult is established primarily through the process of angiogenesis; however, recent studies have demonstrated that endothelial progenitor cells could promote neovascularization,[4] which presents a paradigm in which vasculogenesis contributes to therapeutic neovascularization in the adult. For example, the Transplantation Of Progenitor Cells And Regeneration Enhancement in Acute Myocardial Infarction (TOPCARE-AMI) trial indicated that circulating endothelial progenitor cells could improve left ventricular ejection fraction in patients after myocardial infarction by improving neovascularization.[5] Recent studies have demonstrated that embryonic stem cells (ES cells) can also differentiate into functional endothelial cells (ES-ECs) through the vasculogenesis process.[6,7] Bioluminescence imaging showed longitudinal survival of transplanted ES-ECs, whereas echocardiography demonstrated functional improvement that arose from increased neovascularization.[8] The harnessing of vasculogenesis has the potential to revolutionize regenerative medicine but is contingent on a means to regulate cellular differentiation.

Although the molecular mechanisms underlying vasculogenesis are increasingly being elucidated, limited knowledge exists on the role of the cellular glyco-microenvironment in the process. Indeed, angiogenic factors such as fibroblast growth factor-2 and vascular endothelial growth factor were shown to bind to heparan sulfate glycosaminoglycans (HSGAGs), a key component of the glyco-microenvironment.[9,10] Similarly, in a recent study, decreased *N*-sulfation of HSGAG chains was found to reduce platelet-derived growth factor-BB–induced pericyte recruitment during vascular development.[11] In the present study, we focused on elucidating the cross talk between HSGAGs-glycome and the transcriptome in regulating vasculo-genesis, specifically the differentiation of ES cells into endothelium. HSGAGS are linear *N*- and *O*-sulfated biopolymers made of disaccharide units covalently linked with glycosylphosphatidylinositol-anchored or secreted proteins. They are posttranslationally sulfated in the Golgi apparatus by various glycosynthetic enzymes, of

NIH-PA Author Manuscript

NIH-PA Author Manuscript

NIH-PA Author Manuscript

which the *N*-deacetylase/*N*-sulfotransferases (NDSTs) are rate-limiting. We demonstrate that both the expression of the glycosynthetic enzyme NDST1 and the sulfation of HSGAGs increase during vasculogenesis. Furthermore, pharmacological modulation of the sulfation pattern or knockdown of NDST1 blocked vasculogenesis, which was rescued by the addition of exogenous HSGAGs. We confirmed these findings in vivo in larval zebrafish, in which downregulation of NDST1 resulted in impaired vascular development. Finally, we identified several downstream pathways that may mediate the regulation of vasculogenesis by HSGAGs. The present study reveals the exciting potential of harnessing defined cellular glyco-microenvironments for directed differentiation of precursor cells into adult tissue in vitro and in vivo.

Methods

Cell Culture

Murine ES cells (129 substrain), obtained from ATCC (Manassas, Va), were differentiated in leukemia inhibitory factor–negative media by seeding cells at a density of 1600 cells/cm^2 under ultralow attachment conditions to promote embryoid body formation. On specific days, equal number of cells were taken from each dish and subjected to real-time polymerase chain reaction (RT-PCR), Western blotting, and immunohistochemistry to monitor the expression of endothelial cell markers.

Enzymatic and Chemical Modification of Glycocalyx

ES cell-surface HSGAGs were modified by treatment with 10 mU/mL of either heparinase I, heparinase III, or sodium chlorate. At the end of the experiments, cells were collected, washed in PBS, and analyzed for endothelial differentiation by RT-PCR, immunoblotting, and immunohistochemistry. HSGAG modification was characterized with capillary electrophoresis.

Isolation and Compositional Analysis of ES Cell-Surface HSGAGs

Cells were trypsinized for 30 minutes at 37°C to harvest cell-surface HSGAGs. Cells were counted to normalize for cell number for subsequent capillary electrophoresis analysis. HSGAGs were purified with an ultrafree DEAE column. Eluted fragments were concentrated with Centricon filters (molecular weight cutoff of 3 kDa; Millipore Corp, Billerica, Mass), freeze-dried overnight, and then digested at 30°C by incubation with 3 mIU each of heparinase I, II, and III. Digested glycosaminoglycan fragments were analyzed with an Agilent 3-dimensional capillary electrophoresis system with a 72-cm extended light path capillary with a 75-μm inner diameter (Agilent Technologies, Santa Clara, Calif). Negative polarity separation was monitored at 235 nm in 50 mmol/L Tris, 10 mmol/L dextran sulfate buffer, pH 2.5. Peaks were assigned by comparison with standards.

Short Hairpin RNA Lentivirus Infection

To selectively knock down NDST1 and forkhead box O3a (FOXO3A) in ES cells, we infected cells using short hairpin RNAs (shRNAs) complementary to NDST1, FOXO3A, or green fluorescent protein (GFP; a gift from Nir Hacohen, Center for Immunology & Inflammatory Diseases, Massachusetts General Hospital, Boston, Mass). These shRNA are

NIH-PA Author Manuscript

NIH-PA Author Manuscript

NIH-PA Author Manuscript

inserted in replication-deficient lentiviruses and possess a puromycin-resistant gene, which allows for selection of infected cells. Briefly, 24-hour-old embryoid bodies were infected with viruses at 1 to 5 multiplicities of infection in the presence of polybrene transfection reagent overnight. Fresh medium was replenished every 3 days. RNA was harvested at specific time points after infection and subjected to RT-PCR, as described in the online-only Data Supplement.

Zebrafish Studies

Zebrafish [TübingenAB and tg(Fli:eGFP)] embryos were maintained in standard E3 solution buffered with HEPES 2 mmol/L. A splice donor morpholino was used to inhibit the expression of zebrafish NDST1. The morpholino sequence was based on the 8 overlapping 3′-exons of 3 predicted open reading frames, each with >50% identity to human NDST1 on the zebrafish genome assembly (Zv6 on the Sanger Institute Ensemble, Cambridge, United Kingdom; GenBank accession numbers XP_699032, XP_695253, and XP_691043). The exon-3 splice donor morpholino was predicted to lead to splicing of exon 2 to exon 4. Scrambled morpholinos were used as a control. Increasing concentrations of morpholinos were injected into 2-cell-stage embryos with a constant volume of 4.6 nL with a Nanoject II (Drummond Scientific, Broomall, Pa). To test the patency of vessels, 4.6 nL of 10% tetramethylrhodamine-labeled 40-kDa dextran (Molecular Probes, Carlsbad, Calif) was injected into the cardiac venous sinus. Bright-field and fluorescence images of the embryos were captured with a Nikon SMZ1500 stereomicroscope and a SPOT Flex camera (Diagnostic Instruments, Inc, Sterling Heights, Mich). Image sequences were obtained with the same setup and exported as movies to match live flow patterns. All procedures were approved by Harvard University's Institutional Animal Care and Use Committee.

Affymetrix Oligonucleotide Gene Arrays

Embryos injected with NDST1 morpholino and their wild-type siblings were harvested at the 6- and 20-somite developmental stages and 24 hours after fertilization (hpf). Total RNA was extracted with TRIzol reagent (Invitrogen, Carlsbad, Calif) and purified with Qiagen RNeasy columns (Qiagen, Valencia, Calif). Hybridization to Affymetrix zebrafish genome arrays and data acquisition were performed at the Harvard Medical School Partners Healthcare Center for Genetics and Genomics. Quality control was done with GeneChip Operating Software (GCOS; Affymetrix, Santa Clara, Calif) and DNA-Chip Analyzer (dChip).[11a] Acquired probe-level data were normalized via the robust multichip average method, and mean log 2 expression intensities from triplicate experiments were used in subsequent differential analysis. Local pooled error and ANOVA differential expression testing were performed in S-Plus (Tibco Software, Palo Alto, Calif), with $P<0.05$ and Bonferroni and Benjamini-Hochberg corrections applied to define significant genes and limit false-positive results, respectively. Regulated transcripts were also investigated by use of a modified *t* test, the R version of the Cyber-T algorithm. Gene pathways based on transcripts regulated for both the robust multichip average method and MAS5 data at each of the 3 time points by the Cyber-T and fold-change criteria described above were defined with Cell Illustrator software and Ingenuity Pathways Analysis (Ingenuity Systems, Inc, Redwood City, Calif). Independent component analysis was performed with MATLAB software (The MathWorks, Natick, Mass; see online-only Data Supplement). Affymetrix

NIH-PA Author Manuscript

NIH-PA Author Manuscript

NIH-PA Author Manuscript

probe sets were annotated on the basis of gene symbols available from the Affymetrix Netaffix World Wide Web site, Entrez Gene, Unigene, GenBank, and the Boston Trans-NIH Zebrafish Genome Initiative. Undefined transcripts are identified by Affymetrix probe IDs. A subset of the differential transcript abundance was confirmed with RT-PCR.

Statistical Analysis

All results were expressed as mean±SEM of at least triplicate samples. Statistical comparisons were obtained with 1-way ANOVA followed by Newman-Keuls post hoc test. Tests were performed with PRISM software (GraphPad Software, San Diego, Calif). Statistical comparisons between 2 groups were obtained by Student *t* test. $P<0.05$ was considered significant.

Results

ES Cells Differentiate Into Endothelial Cells

In the present study, we selected the well-characterized embryonic stem cell–embryoid body (ESC-EB), which closely mimics the in vivo maturation process, as an in vitro model to study vasculogenesis. When grown under ultralow adherent conditions in the absence of leukemia inhibitory factor, ES cells start forming solid morula-like structures within 2 days, which progressively increase in size and finally become cavitated (Figure 1B). As shown in Figure 1A, expression levels for endothelial cell markers such as VE-cadherin, VEGFR2 (vascular endothelial growth factor receptor-2), von Willebrand factor, Tie-2, and angiopoietin-2 increased, whereas expression of the stem cell marker Oct 4 decreased progressively over a 10-day period, consistent with differentiation toward vascular endothelial cells. Confocal imaging after immunolabeling of the ESCEBs for von Willebrand factor revealed a negligible signal at day 3 that progressively increased with time (Figure 1B). These findings are consistent with previous reports[12] in which an increase in endothelial cell markers was observed only after day 3 of differentiation. Hemangioblast precursors are first established at this time point, which coincides with the onset of vasculogenesis in the mouse embryo.[13]

HSGAG Synthesis Is Upregulated During ES Cell Differentiation

Differentiation of ES cells into endothelial cells was paralleled by an increase in NDST1 transcripts and protein, which is a key regulator of the sulfation modification of the nascent HSGAG chain (Figure 1C and 1D).[14] To investigate the functional implication of NDST1 expression, we analyzed the compositional changes in cell-surface HSGAG during ESC-EB differentiation using reverse-polarity capillary electrophoresis. Interestingly, there was an increase in the higher-order sulfated HSGAGs fragments during ESC-EB differentiation (Figure 1E), which indicates an involvement of the glycocalyx in the vasculogenic process.

HSGAGs Modulate Differentiation of ES Cells Into Endothelial Cells

HSGAGs are biopolymers of the disaccharide units uronic acid and glucosamine that can be sulfated at 3 residues (Figure 2A). Treatment with sodium chlorate indirectly blocks the sulfation of HSGAG by competitively inhibiting the formation of 3′-phosphoadenosine-5′-phosphosulfate, the high-energy sulfate donor in cellular sulfation reactions.[15] As shown in

NIH-PA Author Manuscript

NIH-PA Author Manuscript

NIH-PA Author Manuscript

Figure 2B, capillary electrophoresis of cell-surface HSGAGs demonstrates the absence of sulfated disaccharide peaks after 7 days of treatment with sodium chlorate compared with untreated control cells. This inhibition was paralleled by a concentration-dependent decrease in protein expression of the endothelial cell marker von Willebrand factor (Figure 2C). Interestingly, the expression of this endothelial cell marker was restored in part by the addition of exogenous heparin (Figure 2D), which establishes a causal link between HSGAGs and endothelium formation de novo. This was further validated by treatment of the differentiating cells with heparinase I and III, which digest the HSGAGs at regions of high and low sulfation, respectively,[16] and which resulted in significant downregulation of endothelial cell markers (Figure 2E through 2H; online-only Data Supplement Figure I). To further confirm the role of HSGAGS in ES differentiation into endothelial cells, we knocked down the HSGAG-modifying enzyme NDST1 in ES cells using NDST1 shRNA. As shown in Figure 2I, this resulted in 80% knockdown of NDST1, which translated into a significant reduction of the endothelial markers Tie-2, von Willebrand factor, and angiopoietin-2, directly implicating NDST1 in the differentiation of ES cells toward endothelial lineage.

Suppression of NDST1 Leads to Aberrant Vasculature Formation in Zebrafish Embryo

To validate the present in vitro results in an in vivo system, we adopted a strategy wherein we genetically manipulated HSGAG synthesis in zebrafish embryos. BLAST (Basic Local Alignment Search Tool) analysis revealed a zebrafish ortholog for NDST1 on chromosome 21 (Figure 3I). Given a variety of predicted ATG initiation sites at this locus, a splice donor morpholino was designed for the third exon of the shared 3′-end exons common to all 3 predicted transcripts. To confirm the effectiveness of this morpholino, we designed specific primers for RT-PCR of RNA prepared from injected and control 72-hpf embryos. Sequencing of the subcloned fragments confirmed altered splicing that resulted from a premature stop codon. To confirm that the morpholino resulted in the attenuation of HSGAG sulfation, we harvested the cell-surface HSGAGs from 24-hpf embryos and subjected them to compositional analysis using capillary electrophoresis. As shown in Figure 3 (II), NDST1 knockdown resulted in a significant reduction in sulfated disaccharides.

As seen in Figure 3 (III), morpholino-induced knockdown of NDST1 resulted in concentration-dependent aberrant formation of dorsal aorta, caudal vein, and intersegmental vessels, which contributed to the shortened, dysmorphic tails. Although higher concentrations of the morpholino resulted in complete ablation of blood flow beyond the cloacae that resulted in dysmorphic tails, lower concentrations produced more proximal confluence of the dorsal aorta and posterior cardinal vein. Although lower concentrations induced vascular abnormalities, no shortening of the tail was observed, which suggests that the dysmorphic tail was a secondary result of the primary abnormal vascularization. In these cases, stagnant blood cells were found in the space usually occupied by the caudal vein plexus and moved synchronously with the heartbeat (Figure 3 [IIIB]; online-only Data Supplement Movie I). These findings were consistent in both the TübingenAB and tg(Fli:GFP) embryos. Decreased vascular blood flow in zNDST1 embryos was associated with a smaller vessel lumen, evident after injection of 40 kDa of tetramethylrhodamine-labeled dextran.

NIH-PA Author Manuscript

NIH-PA Author Manuscript

NIH-PA Author Manuscript

Exogenous Sulfated HSGAGs Rescues Impaired Vascular Phenotype

To test whether exogenous sulfated HSGAGs induce recovery of vascular phenotype, we treated NDST1 knockdown cells with heparin, which is a highly sulfated HSGAG analog. As shown in Figure 4, treatment with heparin increased the endothelium-specific transcripts. Furthermore, heparin induced a partial recovery of the phenotype in NDST1-knockdown zebrafish (Figure 4B).

Glycocalyx Modifications Modulate Transcriptome Signatures in Developing Zebrafish Embryo

To elucidate glycocalyx-mediated effects on transcriptome regulators of vasculogenesis, we performed global gene-expression analysis of zNDST1 morphants and wild-type siblings at the 6-somite, 20-somite, and 24-hpf time points, which correspond with significant stages of zebrafish vessel development (migration of angioblasts to the midline, major lateral vessel formation, and intersegmental angiogenesis).[17] The local pooled error method was used to identify differentially expressed transcripts between zNDST1 mutants and wild-type siblings at all 3 developmental stages, which revealed 218 significant transcripts (corrected *P* value <0.05, fold-change <0.75 or >1.25; online-only Data Supplement Table I). Hierarchal clustering with a Euclidean distance metric demonstrated distinct temporal expression patterns in the top 50 transcripts (Figure 5A). Independent component analysis confirmed our local pooled error analysis, with 93% of the transcripts that were identified as being differentially expressed by the local pooled error analysis also being in the top 0.5% of transcripts that contributed to the NDST1-associated ICA component 2 (Figure 5B). This Independent Component Analysis component 2 additionally identified a further 34 genes associated with NDST knockdown (online-only Data Supplement Table V). ANOVA analysis of MAS5-normalized data was used to define significant changes in gene transcription after comparison of all developmental stages (Benjamini-Hochberg corrected *P* value <0.05; online-only Data Supplement Table II). Notably, a greater number of significant transcripts were found in the 20-somite stage (619) than in the 6-somite stage (67) or at 24 hpf (119), as shown in Figure 5C. Regulated genes significant for cell signaling, transcription factors, cell proliferation/differentiation, protein stability, apoptosis, and matrix interactions are highlighted in Figure 5D. Finally, the data were log base 2 transformed, normalized by both the MAS5 and robust multichip average methods, and then analyzed with Cyber-T ($P \leq 0.05$, mean fold-change of ≤2 between NDST1 morphant and wild type; online-only Data Supplement Tables III and IV). As with the ANOVA method, after this analysis, the 20-somite stage had the most differentially regulated transcripts, although many overlapping transcripts existed among the different stages (Figure 6A). Pathway analysis based on the regulated transcripts for each developmental stage revealed interconnected networks that regulate apoptosis, differentiation, cell matrix, and cell-cell interaction (Figure 6B through 6D).

Discussion

In the present study, we focused on the roles of the glycosaminoglycan component of the cell-surface glycome in modulating vasculogenesis. As the first step, we recapitulated vasculogen esis from ESC-EBs. The primary vascular plexus formed in the embryonic body

NIH-PA Author Manuscript

NIH-PA Author Manuscript

NIH-PA Author Manuscript

undergoes remodeling from day 6 or 7 onward via sprouting angiogenesis.[12,13] Interestingly, comparison of the compositional analysis of the cell-surface HSGAGs of a day 3 and a day 7 ESC-EB revealed distinct profiles that led to an increase in highly sulfated disaccharide residues with differentiation. These sulfate residues are introduced into the nascent polymer through a series of sequential enzyme-induced modifications. The bifunctional activity of the NDST family appears to be a key regulator in this process, because most of the other modifications, namely, C5 epimerization and 2O, 3O, and 6O sulfations, predominate around the *N*-sulfated regions. Interestingly, both mRNA transcripts and total NDST1 protein levels were upregulated during vasculogenesis, which could explain the increased sulfation of the HSGAG polymer. There are 4 isoforms of NDST with distinct tissue distribution,[18] with only the NDST1 and NDST2 isoforms being expressed in vasculature.[19] In a separate study, Johnson et al[20] had demonstrated a similar upregulation of the NDST4 isoform when ESC-EBs were directed to differentiate toward a neural lineage. These observations implicate HSGAG synthetic enzymes in the differentiation process, which indicates that the postpolymerization modifications introduced in the nascent chains could play critical roles in the differentiation process toward specific lineages.

To test this hypothesis further, we used a morpholino-based approach to knock down the expression of NDST1 in a developing zebrafish embryo model, which has emerged as an excellent system to study vasculogenesis because the transparent embryo allows for real-time functional monitoring of the evolving vasculature.[21] In a previous study, genetic perturbation of HSGAG synthesis had resulted in early developmental defects, including failure to differentiate mesodermal precursors of the endothelium,[22,23] which prevented further characterization of vasculogenesis in these studies. This limitation was overcome with the zebrafish model, in which real-time monitoring of the embryo revealed that the oligonucleotide-induced knockdown of NDST1 resulted in reduction of HSGAG sulfation, which led to abnormal vasculature and stunting of the tail, consistent with our hypothesis that the glycocalyx is implicated in vasculogenesis. Additionally, shRNA knockdown of NDST1 significantly suppressed the expression of endothelial markers in the embryoid bodies. This was further supported by the fact that treatment of the differentiating embryoid bodies with heparinase I or III resulted in inhibition of vasculogenesis. Similarly, sodium chlorate, which prevents sulfation of the nascent polymer, also blocked vasculogenesis. This was further validated by the partial recovery of the endothelial phenotype both in the embryoid body and in the zNDST1-knockdown zebrafish after addition of exogenous heparin, a highly sulfated HSGAG analog. These results therefore implicate a causal link between glycome composition and endothelium formation.

In a previous study, we demonstrated that the cellular pheno-type was coregulated by the cross talk between the glycome and the transcriptome.[24] Interestingly, Jakobsson et al[25] demonstrated that HSGAGs expressed on perivascular smooth muscle cells could support the development of capillary structures from NDST1/2$^{-/-}$ embryonic stem cells, which suggests that not just endothelial cell-surface HSGAGs but also the glycocalyx of the surrounding cellular architecture can exert a “bystander effect” in modulating vasculogenesis. We therefore decided to globally knock down NDST1 and study the effect

NIH-PA Author Manuscript

NIH-PA Author Manuscript

NIH-PA Author Manuscript

on the transcriptome, and we developed mechanistic models based on the differentially regulated transcripts that are implicated in neovascularization.

Not surprisingly, a large number of genes that were differentially regulated were those involved in signal transduction and morphogenesis or were transcription factors (see the online-only Data Supplement for details). For example, spleen tyrosine kinase (SYK) was upregulated in NDST1knockdown embryos. SYK is a candidate tumor-suppressor gene that has been implicated in suppression of cyclin D1.[26] It suppresses cell motility by inhibiting phosphoinositide-3 kinase activity and urokinase-type plasminogen activator secretion, which are critical in neovascularization.[27] Interestingly, phosphoinositide-3 kinase also negatively regulates FOXO, which is described below. We also observed downregulation of the *Wnt* receptor, Frizzled, in NDST1-knockdown embryos, as well as another morphogen, the sonic hedgehog (*Shh*). Previous studies in zebrafish have revealed vascular defects in *Shh*-mutant embryos.[28]

Interestingly, despite the implication that HSGAGs are involved in vascular endothelial growth factor, fibroblast growth factor, or platelet-derived growth factor signaling in angiogenesis,[8–10] none of these signals were found to be directly modulated in the NDST1 knockdown embryos. Instead, transcription factor FOXO5 (zebrafish ortholog of FOXO3A) and insulin-like growth factor-2 (IGF2) were found to be consistently upregulated at all 3 time points. In an elegant study, Potente et al[29] demonstrated that an in vivo FOXO3A deficiency increased vessel formation and maturation. We dissected this pathway further in the embryoid body model. As shown in Figure 7, we observed that FOXO3A levels decreased as the cells differentiated into endothelial cells. Interestingly, shRNA-mediated knockdown of NDST1 increased both FOXO3A transcript and protein expression, which suggests that FOXO3A is a downstream signal of glycome modification. Furthermore, shRNA-mediated knockdown of FOXO3A in the embryoid bodies resulted in decreased IGF2 transcripts, which suggests that IGF2 is modulated by FOXO. Indeed, there is evidence of a bidirec tional signaling between IGFs and FOXO.[30] A recent study has demonstrated that the self-renewal and pluripotent properties of ES cells require IGF signaling.[31] In contrast, another study demonstrated that IGF2 is implicated in homing of endothelial progenitor cells.[32] This indicates regulation of IGF activity during differentiation of progenitor cells into endothelial cells, which warrants further studies. Although additional pathways could be coordinating the glycome-transcriptome cross talk in vasculogenesis, the present results clearly implicate the FOXOIGF signaling axis in this process.

In conclusion, we clearly demonstrate the involvement of HSGAGs, key components of cell-surface glycome, in vasculo-genesis. Furthermore, we have elucidated some of the critical downstream pathways that may be implicated in mediating the glycome regulation of vasculogenesis. This study reveals the exciting potential for harnessing defined cellular glycomicroenvironments for directed differentiation of precursor cells for therapeutic neovascularization.

None.

NIH-PA Author Manuscript
NIH-PA Author Manuscript
NIH-PA Author Manuscript

Supplementary Material

Refer to Web version on PubMed Central for supplementary material.

Acknowledgments

Sources of Funding

Dr Sengupta is supported by a Scientist Development Grant from the American Heart Association and a Department of Defense Breast Cancer Research Program Era of Hope Scholar Award. Dr Harfouche is supported by a Canadian Institutes of Health Research postdoctoral fellowship.

References

1. Heart disease and stroke statistics—2007 update: a report from the American Heart Association Heart Statistics Committee and Stroke Statistics Subcommittee. Circulation. 2007; 115:e69–e171. [PubMed: 17194875]
2. Ferrara N, Kerbel RS. Angiogenesis as a therapeutic target. Nature. 2005; 438:967–974. [PubMed: 16355214]
3. Risau W. Mechanisms of angiogenesis. Nature. 1997; 386:671–674. [PubMed: 9109485]
4. Kocher AA, Schuster MD, Szabolcs MJ, Takuma S, Burkhoff D, Wang J, Homma S, Edwards NM, Itescu S. Neovascularization of ischemic myocardium by human bone-marrow-derived angioblasts prevents cardiomyocyte apoptosis, reduces remodeling and improves cardiac function. Nat Med. 2001; 7:430–436. [PubMed: 11283669]
5. Schächinger V, Assmus B, Britten MB, Honold J, Lehmann R, Teupe C, Abolmaali ND, Vogl TJ, Hofmann WK, Martin H, Dimmeler S, Zeiher AM. Transplantation of progenitor cells and regeneration enhancement in acute myocardial infarction: final one-year results of the TOPCARE-AMI Trial. J Am Coll Cardiol. 2004; 44:1690–1699. [PubMed: 15489105]
6. Yamashita J, Itoh H, Hirashima M, Ogawa M, Nishikawa S, Yurugi T, Naito M, Nakao K, Nishikawa S. Flk1-positive cells derived from embryonic stem cells serve as vascular progenitors. Nature. 2000; 408:92–96. [PubMed: 11081514]
7. Levenberg S, Golub JS, Amit M, Itskovitz-Eldor J, Langer R. Endothelial cells derived from human embryonic stem cells. Proc Natl Acad Sci U S A. 2002; 99:4391–4396. [PubMed: 11917100]
8. Li Z, Wu JC, Sheikh AY, Kraft D, Cao F, Xie X, Patel M, Gambhir SS, Robbins RC, Cooke JP, Wu JC. Differentiation, survival, and function of embryonic stem cell derived endothelial cells for ischemic heart disease. Circulation. 2007; 116(suppl):I–46–I-54.
9. Lundin L, Larsson H, Kreuger J, Kanda S, Lindahl U, Salmivirta M, Claesson-Welsh L. Selectively desulfated heparin inhibits fibroblast growth factor-induced mitogenicity and angiogenesis. J Biol Chem. 2000; 275:24653–24660. [PubMed: 10816596]
10. Gitay-Goren H, Soker S, Vlodavsky I, Neufeld G. The binding of vascular endothelial growth factor to its receptors is dependent on cell surface-associated heparin-like molecules. J Biol Chem. 1992; 267:6093–6098. [PubMed: 1556117]
11. Abramsson A, Kurup S, Busse M, Yamada S, Lindblom P, Schallmeiner E, Stenzel D, Sauvaget D, Ledin J, Ringvall M, Landegren U, Kjellén L, Bondjers G, Li JP, Lindahl U, Spillmann D, Betsholtz C, Gerhardt H. Defective N-sulfation of heparan sulfate proteoglycans limits PDGF-BB binding and pericyte recruitment in vascular development. Genes Dev. 2007; 21:316–331. [PubMed: 17289920]
11a. Li C, Wong H. Model-based analysis of oligonucleotide arrays: expression index computation and outlier detection. Proc Natl Acad Sci. 2001; 98:31–36. [PubMed: 11134512]
12. Evans AL, Bryant J, Skepper J, Smith SK, Print CG, Charnock-Jones DS. Vascular development in embryoid bodies: quantification of transgenic intervention and antiangiogenic treatment. Angiogenesis. 2007; 10:217–226. [PubMed: 17577673]
13. Nakagami H, Nakagawa N, Takeya Y, Kashiwagi K, Ishida C, Hayashi S, Aoki M, Matsumoto K, Nakamura T, Ogihara T, Morishita R. Model of vasculogenesis from embryonic stem cells for

NIH-PA Author Manuscript

NIH-PA Author Manuscript

NIH-PA Author Manuscript

vascular research and regenerative medicine. Hypertension. 2006; 48:112–119. [PubMed: 16754788]

14. Grobe K, Ledin J, Ringvall M, Holmborn K, Forsberg E, Esko JD, Kjellén L. Heparan sulfate and development: differential roles of the N-acetylglucosamine N-deacetylase/N-sulfotransferase isozymes. Biochim Biophys Acta. 2002; 1573:209–215. [PubMed: 12417402]
15. Delehedde M, Seve M, Sergeant N, Wartelle I, Lyon M, Rudland PS, Fernig DG. Fibroblast growth factor-2 stimulation of p42/44MAPK phosphorylation and IkappaB degradation is regulated by heparan sulfate/heparin in rat mammary fibroblasts. J Biol Chem. 2000; 275:33905–33910. [PubMed: 10944532]
16. Ernst S, Langer R, Cooney CL, Sasisekharan R. Enzymatic degradation of glycosaminoglycans. Crit Rev Biochem Mol Biol. 1995; 30:387–444. [PubMed: 8575190]
17. Jin SW, Beis D, Mitchell T, Chen JN, Stainier DY. Cellular and molecular analyses of vascular tube and lumen formation in zebrafish. Development. 2005; 132:5199–5209. [PubMed: 16251212]
18. Iozzo RV. Basement membrane proteoglycans: from cellar to ceiling. Nat Rev Mol Cell Biol. 2005; 6:646–656. [PubMed: 16064139]
19. Esko JD, Selleck SB. Order out of chaos: assembly of ligand binding sites in heparan sulfate. Annu Rev Biochem. 2002; 71:435–471. [PubMed: 12045103]
20. Johnson CE, Crawford BE, Stavridis M, Ten Dam G, Wat AL, Rushton G, Ward CM, Wilson V, van Kuppevelt TH, Esko JD, Smith A, Gallagher JT, Merry CL. Essential alterations of heparan sulfate during the differentiation of embryonic stem cells to Sox1-enhanced green fluorescent protein-expressing neural progenitor cells. Stem Cells. 2007; 25:1913–1923. [PubMed: 17464092]
21. Kidd KR, Weinstein BM. Fishing for novel angiogenic therapies. Br J Pharmacol. 2003; 140:585–594. [PubMed: 14534143]
22. Lin X, Wei G, Shi Z, Dryer L, Esko JD, Wells DE, Matzuk MM. Disruption of gastrulation and heparin sulfate biosynthesis in EXT1-deficient mice. Dev Biol. 2000; 224:299–311. [PubMed: 10926768]
23. Stickens D, Zak BM, Rougier N, Esko JD, Werb Z. Mice deficient in Ext2 lack heparan sulfate and develop exotoses. Development. 2005; 132:5055–5068. [PubMed: 16236767]
24. Johnson NA, Sengupta S, Saidi SA, Lessan K, Charnock-Jones SD, Scott L, Stephens R, Freeman TC, Tom BD, Harris M, Denyer G, Sundaram M, Sasisekharan R, Smith SK, Print CG. Endothelial cells preparing to die by apoptosis initiate a program of transcriptome and glycome regulation. FASEB J. 2004; 18:188–190. [PubMed: 14630703]
25. Jakobsson Kreuger J, Holmborn K, Lundin L, Eriksson I, Kjellén L, Claesson-Welsh L. Heparan sulfate in trans potentiates VEGFR-mediated angiogenesis. Dev Cell. 2006; 10:625–634. [PubMed: 16678777]
26. Wang L, Devarajan E, He J, Reddy SP, Dai JL. Transcription repressor activity of spleen tyrosine kinase mediates breast tumor suppression. Cancer Res. 2005; 65:10289–10297. [PubMed: 16288017]
27. Mahabeleshwar GH, Kundu GC. SYK, a protein tyrosine kinase, suppresses the cell motility and nuclear factor kappa B-mediated secretion of urokinase type plasminogen activator by inhibiting the phosphatidylinositol 3′-kinase activity in breast cancer cells. J Biol Chem. 2003; 278:6209–6221. [PubMed: 12477728]
28. Chen JN, Haffter P, Odenthal J, Vogelsang E, Brand M, van Eeden FJ, Furutani-Seiki M, Granato M, Hammerschmidt M, Heisenberg CP, Jiang YJ, Kane DA, Kelsh RN, Mullins MC, Nüsslein-Volhard C. Mutations affecting the cardiovascular system and other internal organs in zebrafish. Development. 1996; 123:293–302. [PubMed: 9007249]
29. Potente M, Urbich C, Sasaki K, Hofmann WK, Heeschen C, Aicher A, Kollipara R, DePinho RA, Zeiher AM, Dimmeler S. Involvement of Foxo transcription factors in angiogenesis and postnatal neovascularization. J Clin Invest. 2005; 115:2382–2392. [PubMed: 16100571]
30. Liu TJ, Lai HC, Ting CT, Wang PH. Bidirectional regulation of upstream IGF-I/insulin receptor signaling and downstream FOXO1 in cardiomyocytes. J Endocrinol. 2007; 192:149–158. [PubMed: 17210752]
31. Bendall SC, Stewart MH, Menendez P, George D, Vijayaragavan K, Werbowetski-Ogilvie T, Ramos-Mejia V, Rouleau A, Yang J, Bossé M, Lajoie G, Bhatia M. IGF and FGF cooperatively

establish the regulatory stem cell niche of pluripotent human cells in vitro. Nature. 2007; 448:1015–1021. [PubMed: 17625568]

32. Maeng Y, Choi H, Kwon J, Park YW, Choi KS, Min JK, Kim YH, Suh PG, Kang KS, Won MH, Kim YM, Kwon YG. Endothelial progenitor cell homing: prominent role of the IGF2-IGF2R-PLCbeta2 axis. Blood. 2009; 113:233–243. [PubMed: 18832656]

NIH-PA Author Manuscript

NIH-PA Author Manuscript

NIH-PA Author Manuscript

NIH-PA Author Manuscript

NIH-PA Author Manuscript

NIH-PA Author Manuscript

CLINICAL PERSPECTIVE

Promotion of neovasculature holds the potential for ameliorating coronary artery disease. The TOPCARE-AMI (Transplantation Of Progenitor Cells And Regeneration Enhancement in Acute Myocardial Infarction) trial indicated that circulating endothelial progenitor cells could improve left ventricular ejection fraction in patients after myocardial infarction. Recent studies have demonstrated that embryonic stem cells can differentiate into functional endothelial cells through vasculogenesis, which results in functional improvement that arises from increased neovascularization. The harnessing of vasculogenesis has the potential to revolutionize regenerative medicine but is contingent on a means to regulate cellular differentiation. In the present study, we demonstrate that the glyco-microenvironment of the stem cell, specifically the sulfated heparan sulfate glycosaminoglycans, plays a critical role in facilitating vasculogenesis. We confirmed these findings in vivo in larval zebrafish, in which desulfation of heparan sulfate glycosaminoglycans resulted in impaired vascular development. The phenotype is rescued with exogenous sulfated heparan sulfate glycosaminoglycans. Finally, we identified several downstream pathways that may mediate the regulation of vasculogenesis by heparan sulfate glycosaminoglycans, including a novel FOXO3A/5-IGF2 signaling pathway. This study reveals the exciting potential of harnessing defined cellular glyco-microenvironments for directed differentiation of precursor cells into endothelial cells, leading to neovascularization.

NIH-PA Author Manuscript
NIH-PA Author Manuscript
NIH-PA Author Manuscript

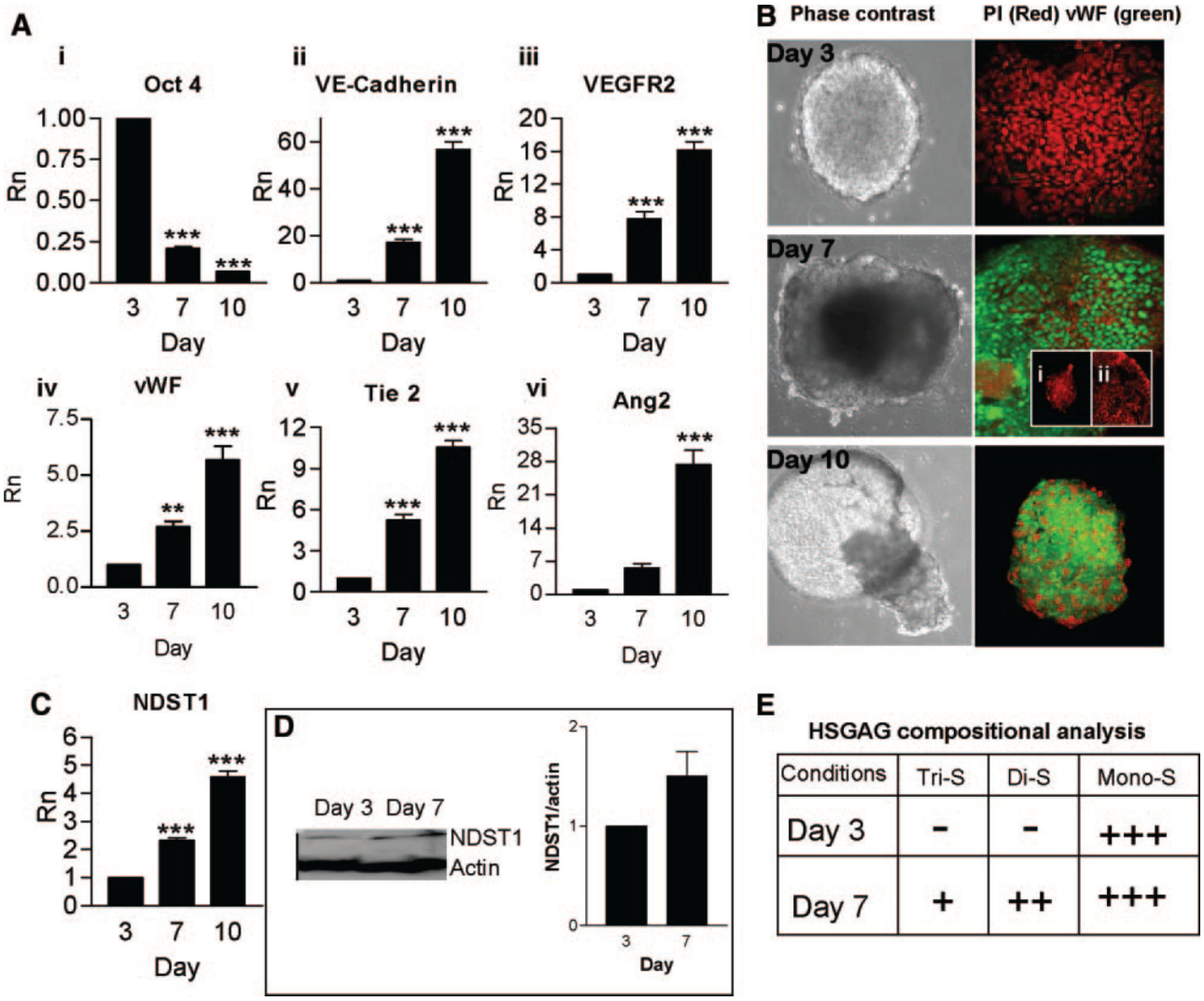

Figure 1.

Differentiation of ES cells into endothelium. A, i–vi, Quantification of endothelial cell transcripts (VE-cadherin, vascular endothelial growth factor receptor 2 [VEGFR2], von Willebrand factor [vWF], Tie-2, and angiopoietin-2 [Ang2]) and stem cell marker Oct 4 with RT-PCR. B, Bright-field and confocal images of embryoid bodies stained for vWF confirm differentiation into an endothelial lineage. Images were captured with an LSM510 confocal microscope with a 488-nm wavelength for excitation and emission at 516 nm. Inset (i–ii) represents isotype control and immunohistochemistry without primary antibody as control. PI indicates propidium iodide. C, RT-PCR analysis revealed expression of NDST1 during differentiation. D, Western blot shows expression of NDST1 protein over time in a differentiating embryoid body. E, Compositional analysis of HSGAGs by capillary electrophoresis after heparinase digestion revealed negligible sulfated disaccharides at day 3 compared with day 7, when the vascular precursors had been established. The data are expressed as grades of intensity of signal from the electropherogram. Tri-S indicates trisaccharide; Di-S, disaccharide; Mono-S, monosaccharide; and Rn, normalized reporter. ***P<0.001 compared with day 3 control cells.

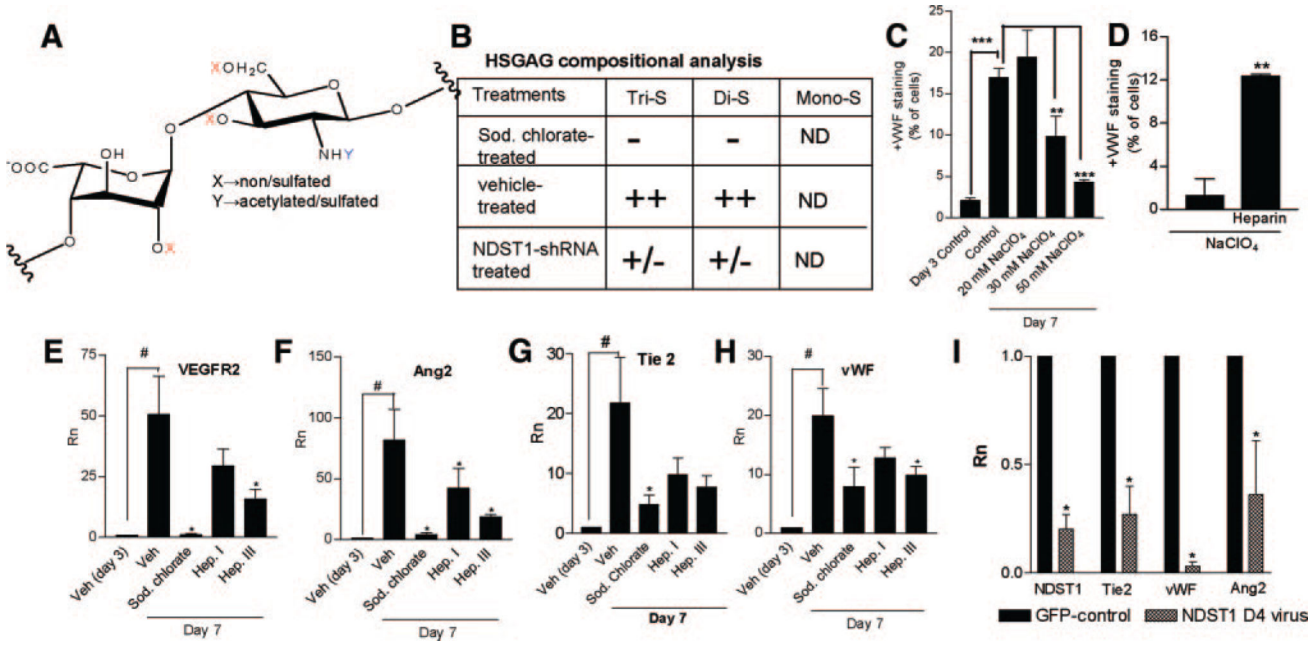

Figure 2.

Pharmacological modulation of HSGAGs regulates vasculogenesis. A, Typical disaccharide building block of HSGAG polymer comprises a uronic acid and a glucosamine. It can be sulfated at residue X and sulfated or acetylated at Y. B, Treatment of ES cells with sodium chlorate (Sod. chlorate) inhibited sulfation of the nascent chain, as seen by capillary electrophoresis. Data are expressed as grades of intensity of signal from the electropherogram. ND indicates nondetectable; Tri-S, trisaccharide; Di-S, disaccharide; and Mono-S, monosaccharide. C, Fluorescence-activated cell sorter analysis for expression of von Willebrand factor (vWF) in sodium chlorate–treated embryoid bodies showed a concentration-dependent inhibition of vasculogenesis (D) that could be reversed with exogenous heparin. E–H, Differentiation of ES cells to endothelial cells was inhibited by treatment with heparinase I or III and sodium chlorate as quantified by monitoring the level of transcripts of endothelial cell markers (vascular endothelial growth factor receptor 2 [VEGFR2], angiopoietin 2 [Ang2], Tie-2, and vWF) with RT-PCR. ***P*<0.05, ***P*<0.01, ****P*<0.001 compared with control. #*P*<0.01 vs day 3. I, NDST1 gene was knocked down in ESC-EBs for 7 days with NDST1 shRNA (gray bars), and gene expression of NDST1 and endothelial markers (Tie-2, vWF, and Ang2) was quantified by RT-PCR. GFP shRNA served as internal control (black bars). **P*<0.05 compared with GFP-shRNA. Veh indicates vehicle; Rn, normalized reporter; and Hep., heparinase.

NIH-PA Author Manuscript NIH-PA Author Manuscript NIH-PA Author Manuscript

NIH-PA Author Manuscript
NIH-PA Author Manuscript
NIH-PA Author Manuscript

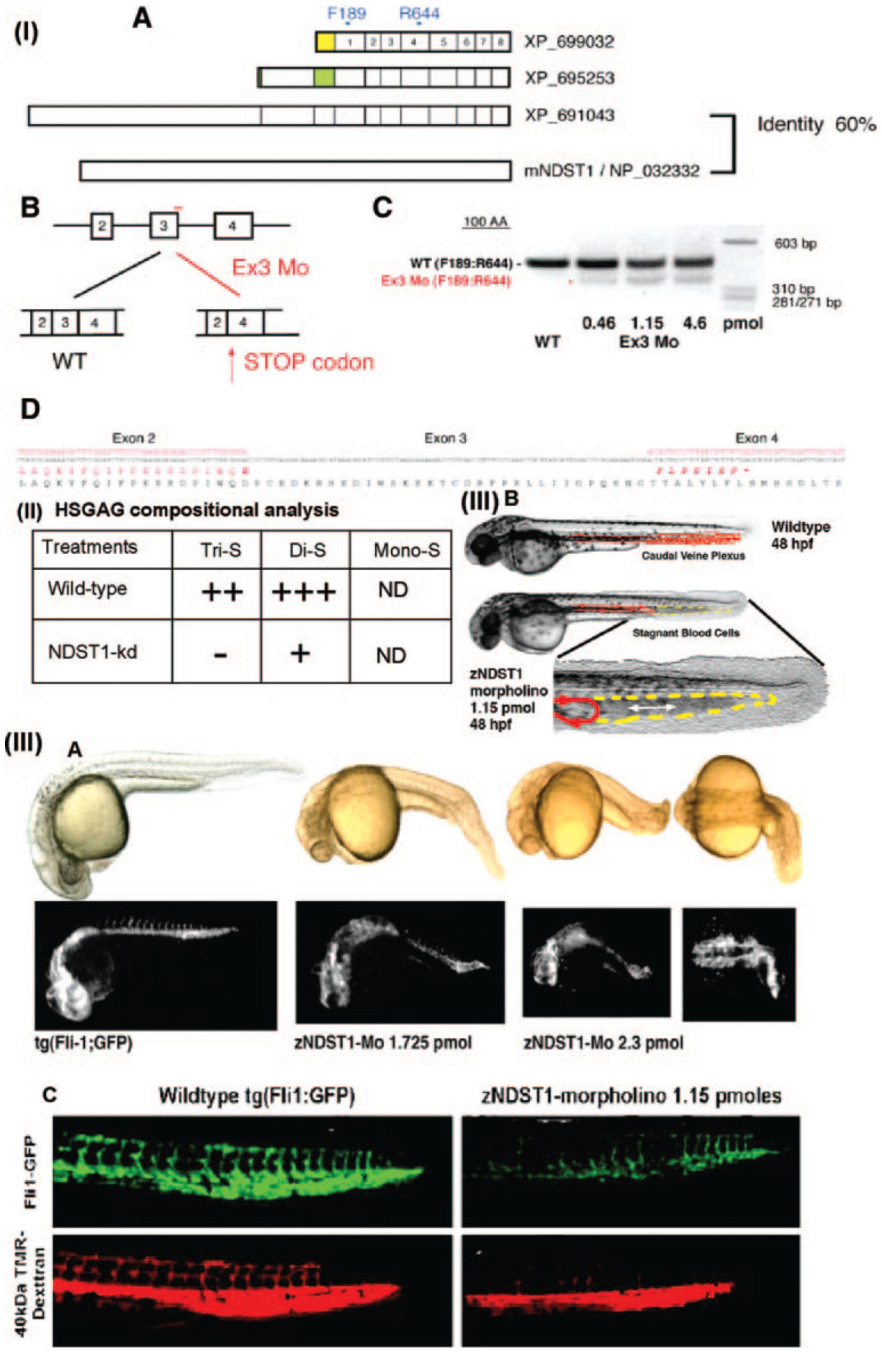

Figure 3.

Morpholino-induced knockdown of NDST1 impairs vasculogenesis in zebrafish embryo. I-A, BLAST analysis revealed 3 zebrafish orthologs for zNDST1 on chromosome 21 with 60% sequence identity to mouse NDST (mNDST). I-B, A morpholino (GTGCATTTAACACTCACCATTCTTC) was designed to block the splice donor site of exon 3 (Ex3 Mo). WT indicates wild type. I-C, RT-PCR confirmed effectiveness of the morpholino in a dose-dependent manner. Sequencing of the subcloned fragments confirmed altered splicing that resulted in a premature STOP codon. II, Capillary electrophoresis of HSGAG profile from wild-type and NDST1 knockdown (NDST1-kd) zebrafish at 24 hpf revealed absence of sulfated disaccharides in the NDST1 knockdown compared with the wild type. Data are expressed as grades of intensity of signal from the electropherogram.

Tri-S indicates trisaccharide; Di-S, disaccharide; Mono-S, monosaccharide; and ND, nondetectable. III-A, Morpholino-injected tg(Fli1;GFP) fish displayed decreased intersegmental vessels and dysmorphic tails in a dose-dependent manner. III-B, Bright-field images of TübingenAB 48-hpf WT fish (top) and 1.15-pmol morpholino–injected fish. Blood cells accumulated in the caudal vein plexus of morpholino-injected embryos. III-C, Top, 54-hpf tg(Fli:GFP) embryos injected with low-dose zNDST1 morpholino displayed weaker density of tail intersegmental vessels. Bottom, 40-kDa tetramethylrhodamine (TMR) injected into WT and knockdown fish revealed smaller lumens in zNDST-injected embryos.

NIH-PA Author Manuscript
NIH-PA Author Manuscript
NIH-PA Author Manuscript

NIH-PA Author Manuscript
NIH-PA Author Manuscript
NIH-PA Author Manuscript

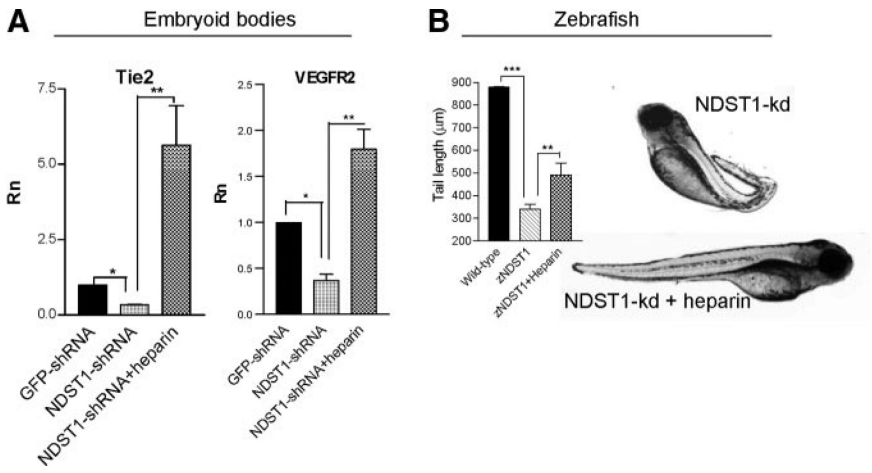

Figure 4.

Exogenous heparin rescues the NDST1-knockdown (NDST1-kd) phenotype. A, RT-PCR data showing transcript levels of endothelial cell markers, Tie-2 and VEGFR2 (vascular endothelial growth factor receptor 2), in differentiating ES cells after shRNA-induced NDST1 knockdown. Incubation with heparin (20 μg/mL) induced recovery of transcript levels after NDST1 knockdown. Data show mean±SE (n=3). B, Injection of heparin in the zNDST1 morpholino-treated zebrafish resulted in partial recovery of the tail phenotype, used as a reporter for vascularization defects. Graph shows mean tail lengths ±SE from 7 to 8 fish per treatment group. **P*<0.05, ***P*<0.01, ****P*<0.001 vs controls.

NIH-PA Author Manuscript
NIH-PA Author Manuscript
NIH-PA Author Manuscript

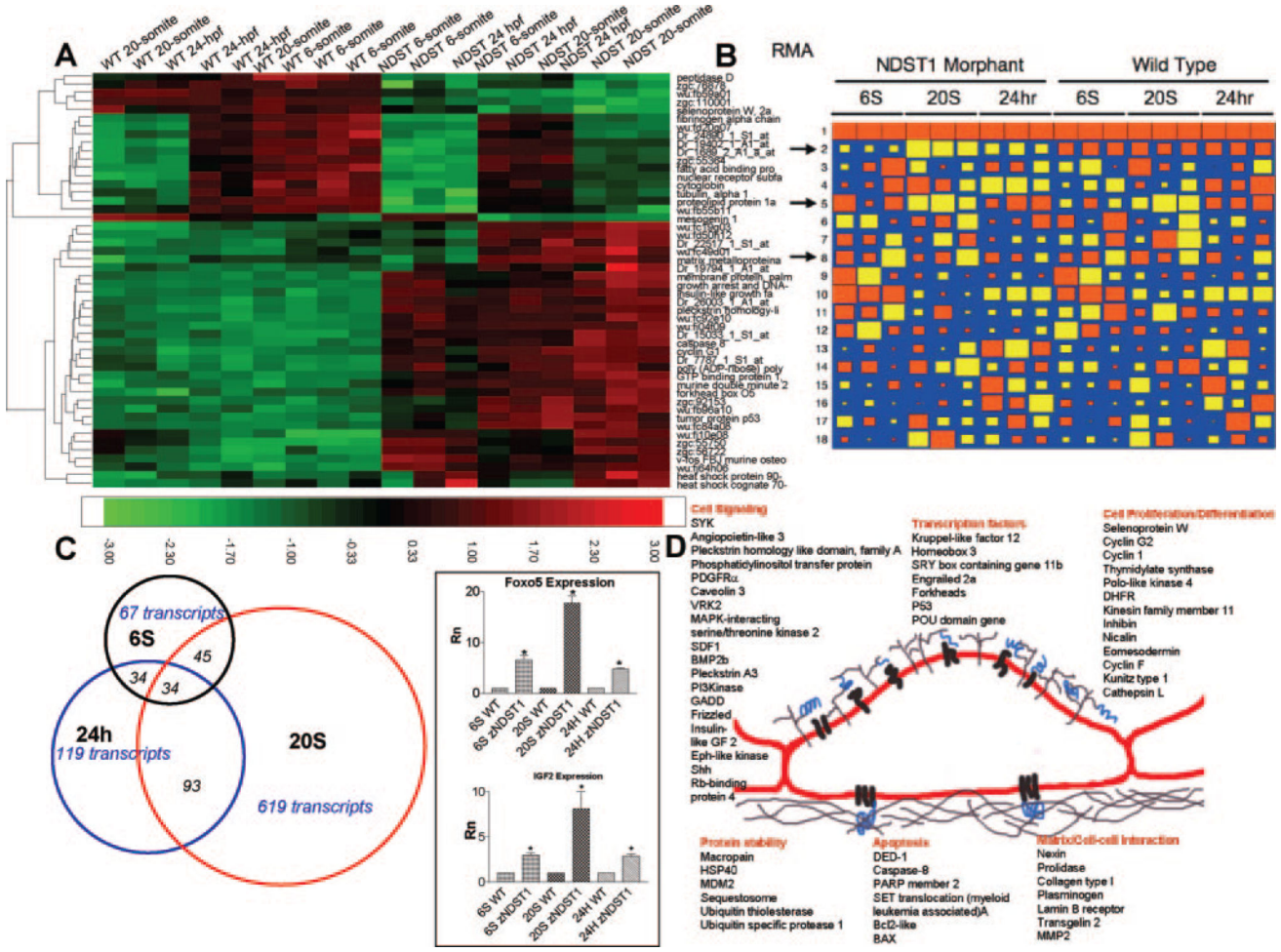

Figure 5.

Temporal transcriptome analysis of wild-type (WT) vs NDST1 knockdown zebrafish. A, Heat map was created from the top 50 significant transcripts according to local pooled error testing in S-Plus software. Differential expression trends are clearly visible between WT and morphant zebrafish embryos at the 6-somite, 20-somite, and 24-hpf developmental stages. Unidentified transcripts are denoted by Affymetrix identification numbers. B, Hinton plot was created with independent component analysis on robust multichip average (RMA) method–normalized expression levels to reveal gene signatures by a method that is independent of parametric statistics. Columns represent chips; rows represent latent gene signatures. Colors and sizes of squares represent the direction (positive or negative) and degree to which each component is represented in each chip. Components specific for the knockdown, developmental stage, and individual biological replicates are arrowed. Ninety-three percent of transcripts identified as differentially expressed by local pooled error analysis were also in the top 0.5% of transcripts that contributed to independent component analysis component 2, which separated WT from NDST1 knockdown. C, ANOVA analysis ($P<0.05$) in S-Plus revealed 67, 619, and 119 regulated transcripts between WT and morphant RNA at the 6-somite, 20-somite, and 24 hpf stages, respectively. The 34 transcripts that overlapped at all developmental stages are highlighted in the Venn diagram. Inset shows confirmation of zebrafish FOXO5 and IGF2 expression by quantitative PCR. D, Cartoon classifying the transcripts that are modulated between WT and NDST1 that are implicated in neovascularization. 6S indicates 6 somite; 20S, 20 somite; and Rn, normalized reporter.

NIH-PA Author Manuscript
NIH-PA Author Manuscript
NIH-PA Author Manuscript

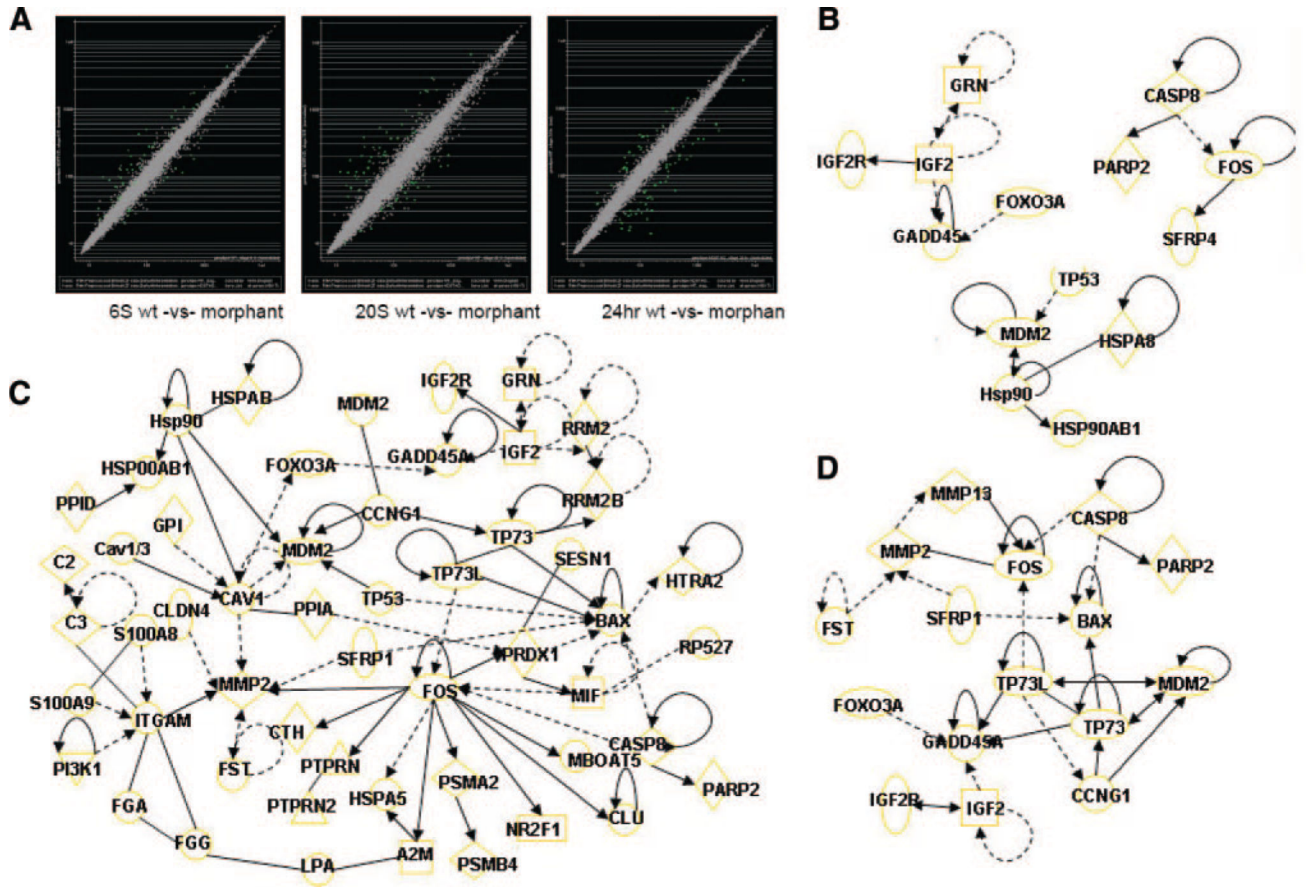

Figure 6.

Pathways implicated in glycocalyx regulation of vasculogenesis. A, At each time point, scatterplots compare mean transcript abundance of the 3 wild-type replicates (*x* axis) with that of the 3 zNDST1 morphant replicates (*y* axis). Those transcripts with $P \geq 0.01$ and fold-change ≤2 by Cyber-T analysis at the 24-hpf time point are highlighted in green for all 3 time points. B, C, and D, Cell Illustrator and Ingenuity pathway analyses were used to construct pathways of significantly regulated transcripts at the 6-somite (6S), 20-somite (20S), and 24-hpf developmental stages according to Cyber-T analysis. A right-tailed Fisher exact test indicated that the likelihood of any of these pathways being constituted by random samples of 67, 619, or 119 transcripts drawn from the Affymetrix microarrays was ≥0.05.

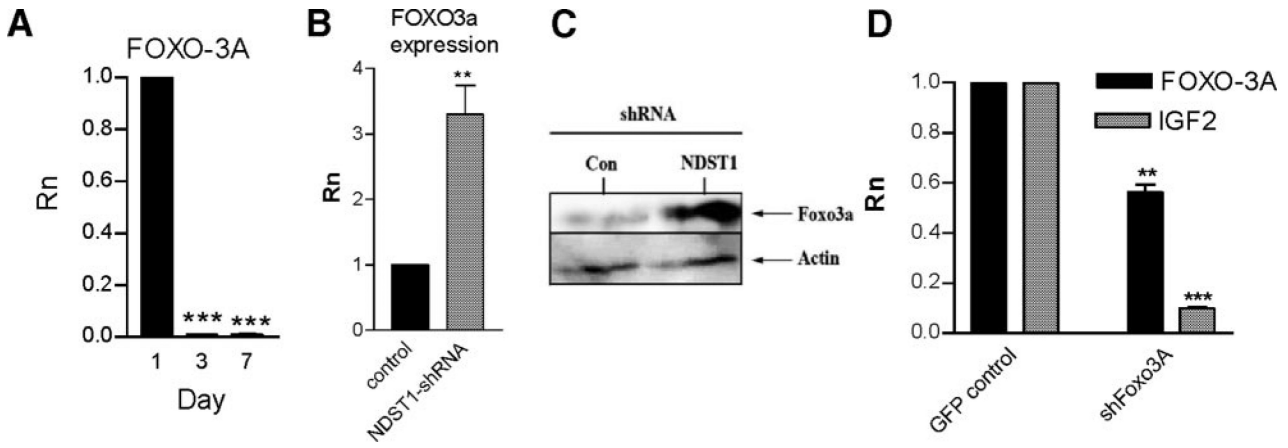

Figure 7.

FOXO3A and IGF signaling in NDST1-mediated vasculogenesis. A, Graph shows expression of FOXO3A transcripts in differentiating embryoid bodies as a function of time. B, Transcript levels of FOXO3A in GFP- and NDST1-shRNA–treated cells were quantified with RT-PCR. C, Western blot showing levels of FOXO3A proteins in control (Con) and NDST1 knockdown ES cells. D, Graph shows transcript levels of IGF2 after NDST1 knockdown in ES cells. E, shRNA-mediated knockdown of FOXO3A resulted in downregulation of IGF2, which indicated that IGF2 was downstream of FOXO3A. shRNA against GFP was used as control. Data shown are mean±SE from at least 3 independent experiments. ***P*<0.01, ****P*<0.001 vs appropriate controls. In graph (a), the day 3 and day 7 groups are statistically compared with day 1. Rn indicates normalized reporter.

NIH-PA Author Manuscript
NIH-PA Author Manuscript
NIH-PA Author Manuscript